Particle induced strand breakage in plasmid DNA

Dang, Hong

CHAPTER 6

Plasmid DNA irradiated by low energy ions

We present some results on the interaction of low energy atomic ions with DNA. The experiments consist of irradiation of dried DNA in vacuum with H, He and C ions at keV energies. The DNA is placed back in solution and analysed by agarose gel electrophoresis. These experiments demonstrate the production of single and double strand breaks. The induction of these lesions can be due to several processes: direct collisions with DNA constituent atoms resulting in displacements, cascade recoil collisions of the constituent atoms, electron transfer processes between the ion and the DNA as well as breaks induced by molecular excitation and secondary electron interactions. To understand the physical process during DNA strand breaks, a Monte Carlo calculation code known as TRIM (Transport of Ions in Matter) was used to simulate energy losses due to nuclear stopping and to electronic stopping. It can be assumed that nuclear stopping plays a significant role in DNA strand breaks in the case of C irradiation. The physical mechanisms of DNA strand breaks induced by a low-energy ion beam are also discussed. We also briefly discuss some aspects of direct and recoil collision processes.

6.1 Low energy ion interactions

Interest in heavy ion cancer therapy has stimulated a large amount of work dealing with the interaction of ions (e.g. C, Ne, etc) with plasmid DNA and cells (see e.g. [20, 138–144]. In the previous chapter, it has been shown that the direct effect dominates DSB induction by swift C^{6+} ions in the Bragg peak region where the particle tracks terminate. The effect of very low energy ions corresponding to this region or of secondary ions produced along the track has only been subject of very few studies [35, 145–149] in part because of the very short range of low energy ions in matter [150]. There are however quite a few research reports about low-energy ion beams interating with isolated building blocks of DNA, in particular nucleobases [151–154]. It is important to note that the characteristics of high and low energy heavy particle collisions are likely to be quite different, because the dominant interaction processes at high energies and low energies are also quite different [155, 156].

In dense media, energetic secondary ions produced along the primary ion track will scatter inelastically over short distances, and may induce complex DNA damage clusters that cannot be repaired by the cell [157].

In the present work we used keV (< 40 keV) H^+ and He^{2+} ions. We also have employed specifically carbon ions because of their relevance to heavy ion therapy [158, 159] and the abundance of carbon in tissue and plasmid DNA. The irradiation target chosen was plasmid DNA (pBR322), a supercoiled circular DNA molecule comprising 4361 base pairs [160].

To conduct a series of experiments involving irradiation of dried plasmid DNA by low energy ions, we used ions directly extracted from a Supernanogan ECR ion source. The probability of inducing single (SSB) or double (DSB) strand breaks in DNA was determined by gel electrophoresis (described in more detail in chapter 2). The experiments indeed show evidence of both SSBs and DSBs induced by low keV energy ions in plasmid DNA. The full results of this experimental campaign are described in the following sections.

6.2 Results

The effects of the low-energy ion impact on plasmid DNA are analysed by means of gel electrophoresis (see chapter 2). The method allows to separate the supercoiled, open cicular and linear forms of the plasmid. When a SSB is induced, the plasmid converts from its nascent supercoiled form (SC) into the open circular form (OC).

The linear form (L) of plasmid DNA occurs as a result of a single DSB. Therefore, the percentage of linear DNA in the samples can be taken as a measure of the frequency of DSB occurrence. Two sequential SSB breaks may also lead to a DSB:

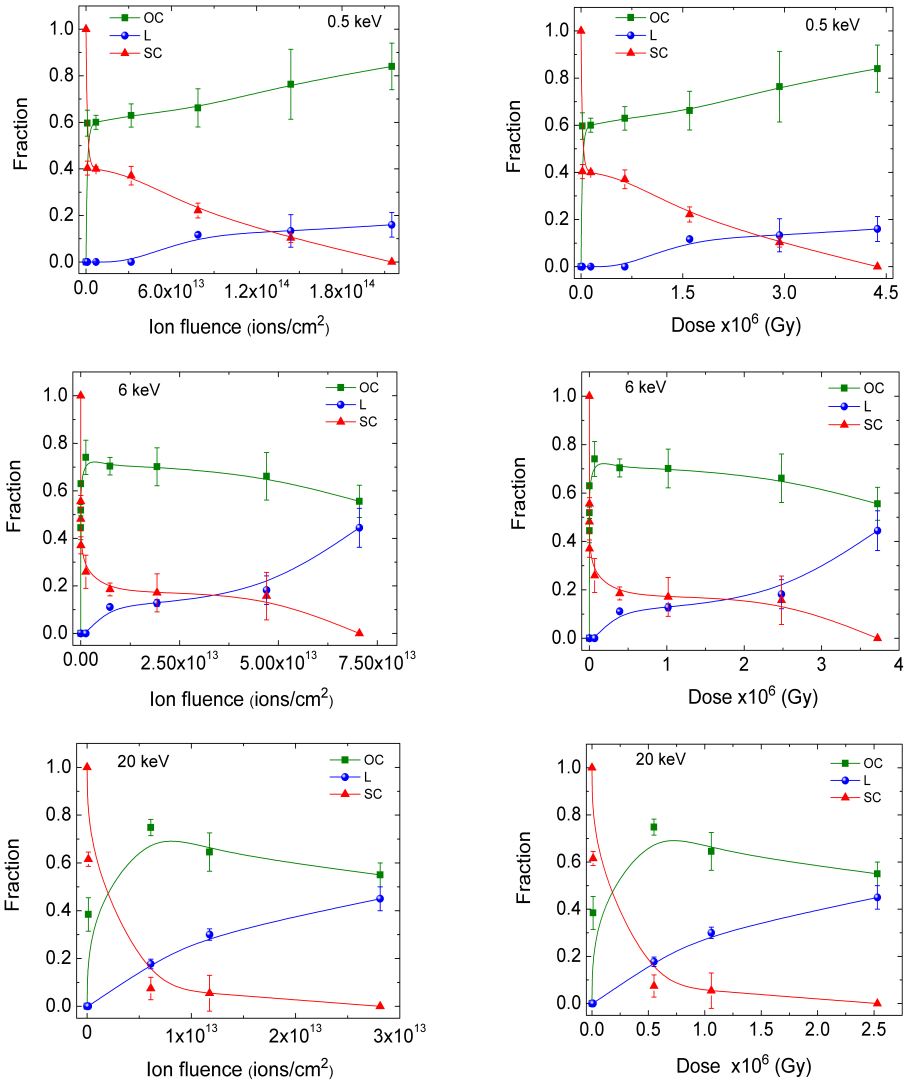

Figure 6.1: *Relative yields of supercoiled (SC), open circular (OC) and linear (L) plasmid DNA after H irradiation as a function of fluence (ions/cm^2) and dose for different energies of H^+. The lines are to guide the eye.*

If the plasmid receives more than one SSB on opposite strands, it is usually still held together by hydrogen bonds. Only very closely spaced SSBs typically within 10 bp distance and on opposite strands result in a DSB [161, 162].

Our samples contain about 500 ng of DNA, *i.e.* about 1.1x10^{11} molecules. Plas-

mid DNA pBR322 has 4361 base pairs and 8722 sites available for SSBs per molecule. Thus for a small number of randomly induced SSBs it is unlikely that two of them occur on opposite strands of the same plasmid within distances short enough to produce a DSB. Therefore, this channel will be neglected in the following

The full sets of results on plasmid DNA breakage induced by H^+, He^{2+}, and $C^{+,2+,4+}$ ions at different kinetic energies are shown in figures 6.1–6.3. The results are presented as function of ion fluence and dose. In order to convert particle fluence to dose the following relationship was used [163]:

$$Dose(Gy) = 1.6 \times 10^{-9} \times LET(keV/\mu m) \times Fluence(ions/cm^2) \times 1/\rho(g/cm^3) \quad (6.1)$$

where LET is the linear energy transfer, and ρ is the density of the target material (usually 1 g/cm^3 for biological samples). Using the SRIM programme (Stopping and range of ions in matter see e.g. [72]), it is possible to calculate the LET of different ions at different energies. The LETs of protons, helium and carbon ions with various initial energies are given in table 6.1.

To obtain the data presented in figures 6.1–6.3, two factors had to be taken care of: 1) The non-irradiated plasmid DNA reference samples which underwent the same treatment as the irradiated samples already contain 4% to 6% of OC plasmids. 2) The penetration depth of the ions into the plasmid thin film depends on the ion and on its kinetic energy. DNA damage only occurs in that layer of the film, that is penetrated by the ions. Consequently, a variable fraction of each sample remains unirradiated and even for high dose, the SC fraction does not reach zero. For the figures we have thus offset the SC fraction at high dose to zero (OC and L fractions were affected accordingly). This subtraction process is to some extent arbitrary: DNA damage is not the only possible process. Additionally, some DNA material may be sputtered from the film leading to a dose-dependent erosion that prevents convergence of the plasmid fractions.

In our experiments, the fluence rate of the ion beam was sufficiently low (about 2 nA/cm^2) that consecutive ion-impacts on the same plasmid–site could be considered independent.

It is obvious from fig. 6.1, that the damage of the plasmid DNA (OC and L) after bombardment by low energy H^+ ions increases as a function of the fluence (ions/cm^2) or dose (Gy). The trend is similar for all H^+ energies under study (0.5, 6, and 20 keV): The OC fraction quickly rises until a maximum is reached from which it monotonically decreases. Essentially the same trend has been observed in the previous chapters: DSB or additional SSB can transfer OC plasmids into the L form.

To reduce the fraction of intact plasmid DNA for instance to 20% fluences of approximately 10^{14}, 10^{13} and 5x10^{12} protons/cm^2 are required for 0.5, 6 and 20 keV,

respectively. However, at 0.5, 6 and 20 keV, 5×10^5, 1.9×10^5 and 1×10^5 protons are required respectively, to deposit a dose of one Gy. Thus, when comparing the data of 0.5, 6 and 20 keV protons as a function of dose, one finds doses of the same order of magnitude.

The same trends are observed for the 6-20 keV He^{2+} ions but lower fluences and doses need to be applied (see fig. 6.2). At variance with the case of H^+ ions, for 20 keV He^{2+} the OC fraction does not reach a local maximum anymore.

For C ions (fig. 6.3) again similar trends are observed. Here, only the 10 keV data show an OC fraction that does not reach a local maximum. Furthermore, much lower doses of less than 0.1×10^6 Gy are needed to induced complete plasmid breakage.

Error bars represent one standard deviation of 3 or 4 independent experiments. The uncertainties in the fluence are less than 5%. The determination of dose relies on calculated LET values which may induce a further uncertainty.

Table 6.1: *LET calculation for H, He and C ions with different energies.*

Ion	Energy (keV)	LET (keV/μm)
H	0.5	18.5
	6	48.2
	20	82.1
He	6	55
	10	63.8
	15	73.6
	20	82.7
C	10	196
	20	209
	40	230

The most important direct observation is that we observe linear DNA implying the creation of double strand breaks, thus demonstrating that low energy ions do produce this type of strong (lethal) damage. For all three different ions, to a small extent multiple double strand breaks occur with increasing dose which is manifest in a broad band in the gel that is due to short linear fragments. It is difficult to estimate the amount of these small fractions exactly. In the analysis we have not included data for extremely high doses where short linear fragments start to play a more significant role.

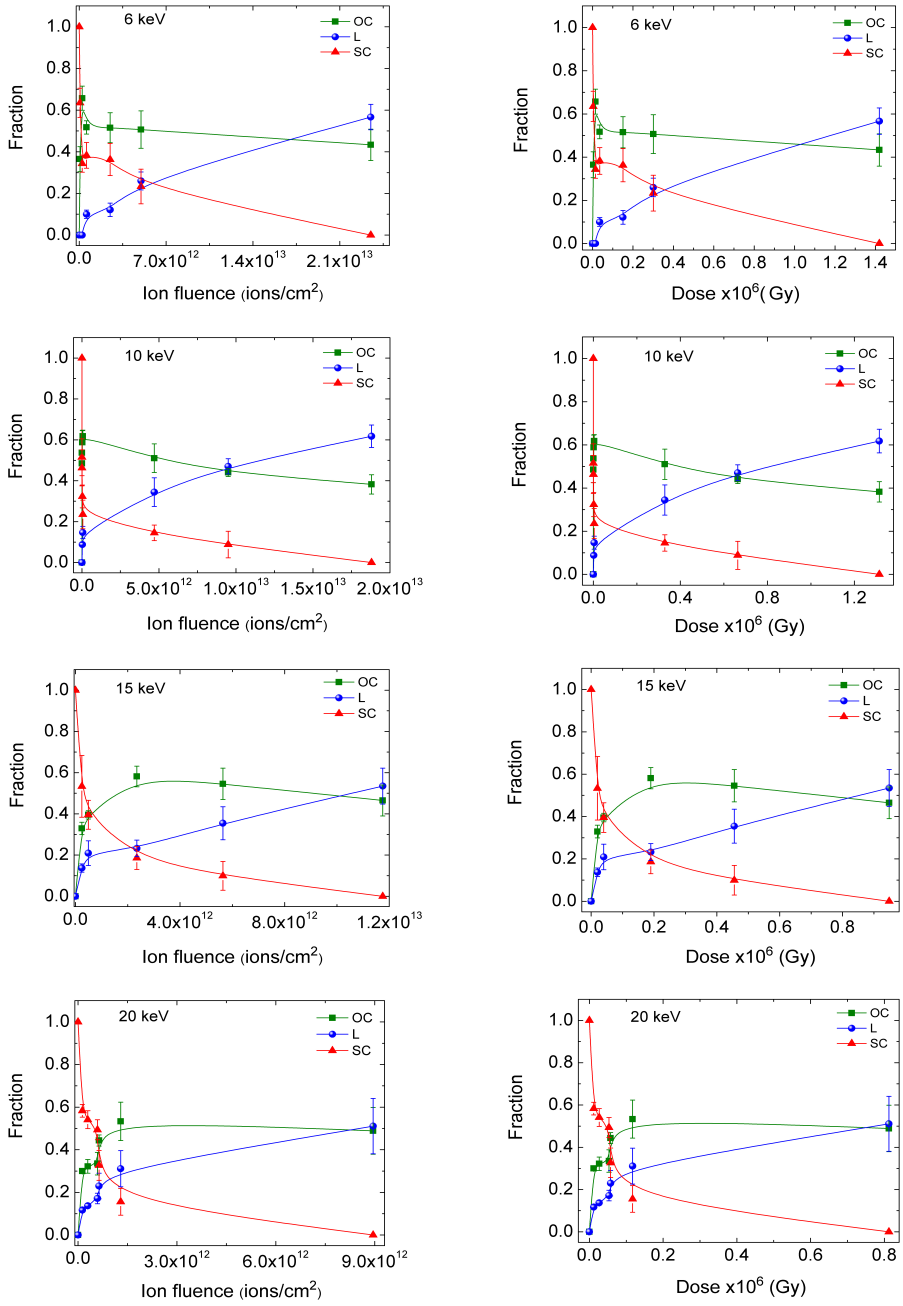

Figure 6.2: *Relative yields of supercoiled (SC), open circular (OC) and linear (L) plasmid DNA after He^{2+} irradiation as a function of fluence (ions/cm^2) and dose for different energies of He. The lines are to guide the eye.*

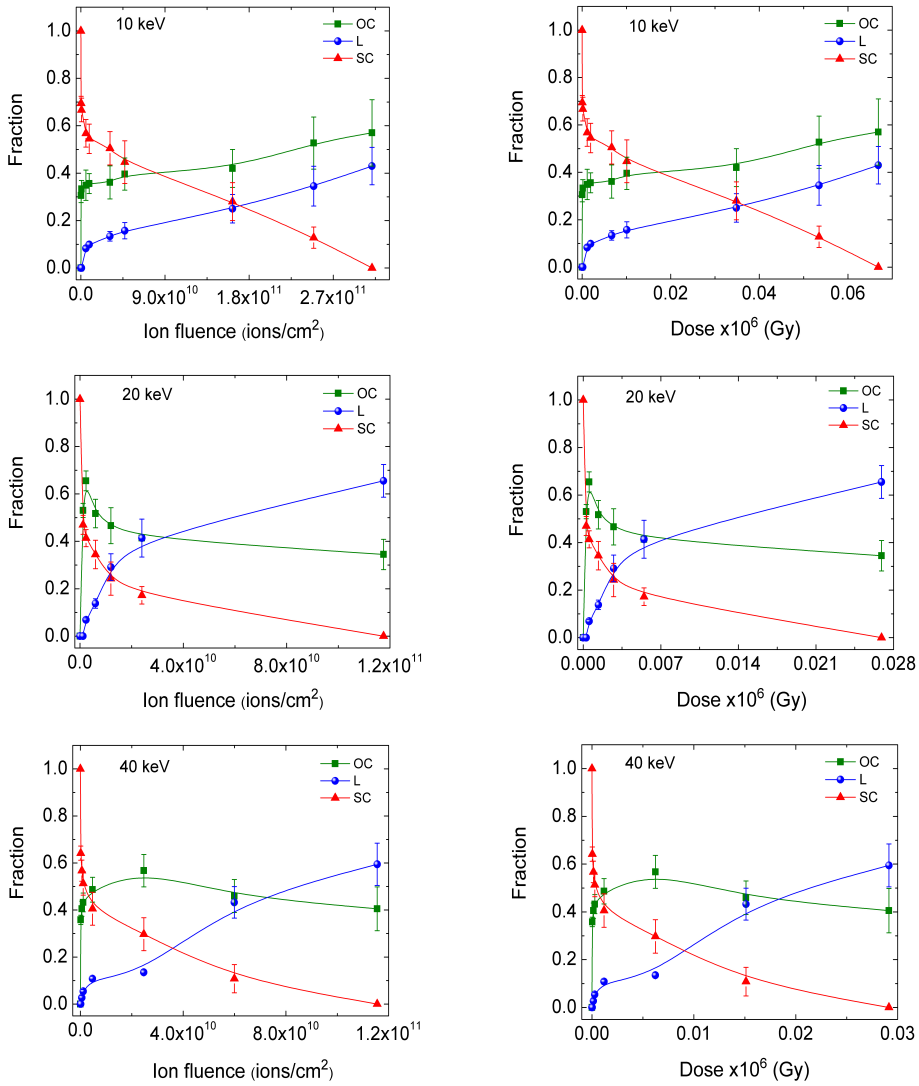

Figure 6.3: *Relative yields of supercoiled (SC), open circular (OC) and linear (L) plasmid DNA after C^{q+} irradiation as a function of fluence (ions/cm^2) and dose. Top: C^{+}, middle: C^{2+}, and bottom: C^{4+}. The lines are to guide the eye.*

6.3 Discussion

Using the same fitting scheme that has been applied to the data in the previous chapters, we can again obtain the SSB yields μ and DSB yields ϕ per plasmid per Gy. The results for the three ions under study are shown in table 6.2. Note, that the fits do not reach the same quality as obtained in the previous chapters. However, the procedure still is an efficient way of transferring the information from figs. 6.1–6.3 into easily comparable numbers. Even though the μ and ϕ values are normalized to

Table 6.2: *SSB per plasmid per Gy (μ) and DSB per plasmid per Gy (ϕ) yields after irradiation with H, He, and C ions at different kinetic energy.*

Ion	Energy (keV)	μ (/plasmid/Gy) $\times 10^{-6}$	ϕ (/plasmid/Gy) $\times 10^{-6}$
H	0.5	0.7 ± 0.4	0.05 ± 0.04
	6	0.6 ± 1.1	0.2 ± 0.1
	20	4.3 ± 4.6	0.4 ± 0.2
He	6	1.6 ± 2.4	0.97 ± 0.79
	10	1.6 ± 3.5	1.35 ± 0.94
	15	4.3 ± 3.7	1.4 ± 0.8
	20	10.2 ± 3.6	2.3 ± 1.2
C	10	35.2 ± 16.1	11.8 ± 4.8
	20	307 ± 22	157 ± 94
	40	109 ± 81	47 ± 20

a /plasmid/Gy scale, large differences between the three ions are obvious. For H^+ and He^{2+}, both μ and ϕ increase with ion kinetic energy. For C^+, the damage is maximum at 20 keV. Furthermore, abolute values for μ and ϕ differ dramatically for the three ions under study.

The increase in damage with ion kinetic energy observed for H^+ and He^{2+} is in line with the trend in LET (see table 6.1). However the LET values for 6 - 20 keV hydrogen and helium ions are very similar so the LETs alone do not explain why helium ions are much more efficient in creating strand breaks than protons.

Carbon ions have a higher LET than hydrogen and helium ions and indeed produce more strand breaks. On basis of the LET values for 10 - 40 keV carbons (table 6.1) one expects no large differences between 10, 20 and 40 keV energy. But clear differences between 10 and 20 and 40 keV are observed.

At present there is no accurate description of the damage mechanism at low

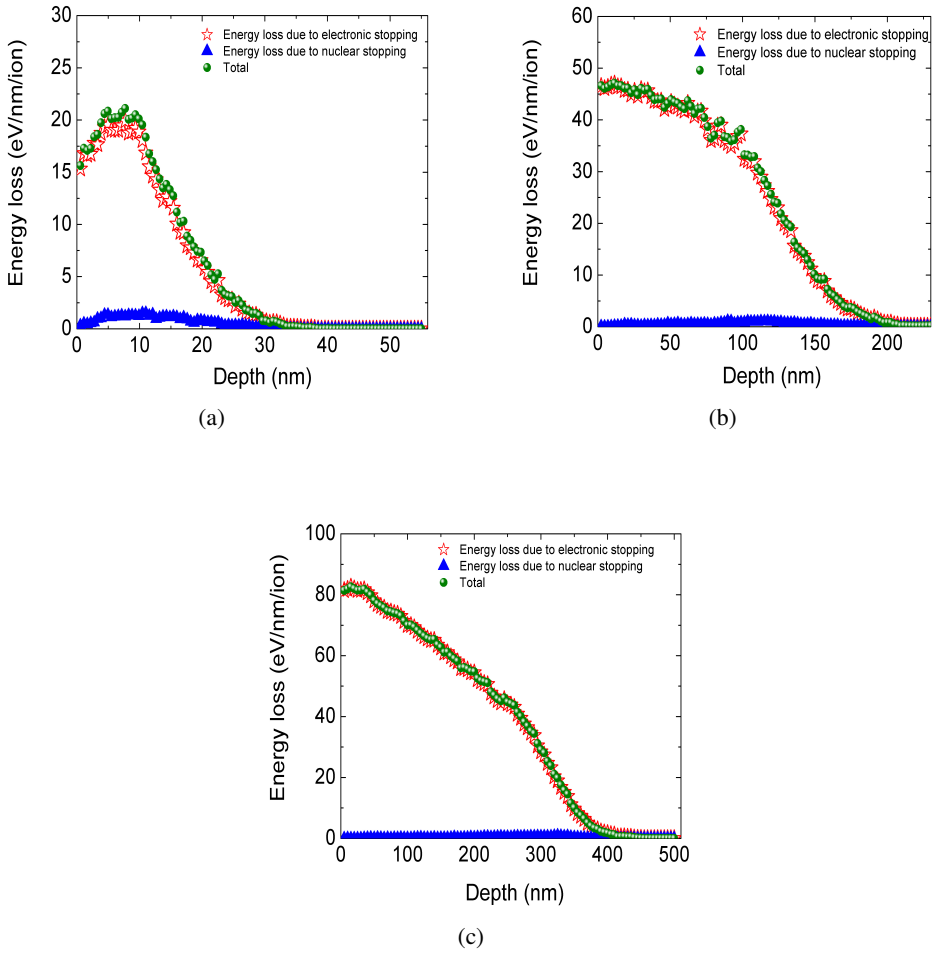

Figure 6.4: *Energy deposition of (a) 0.5-keV, (b) 6-keV, and (c) 20-keV Hydrogen ions implanted into plasmid DNA calculated by the TRIM programme.*

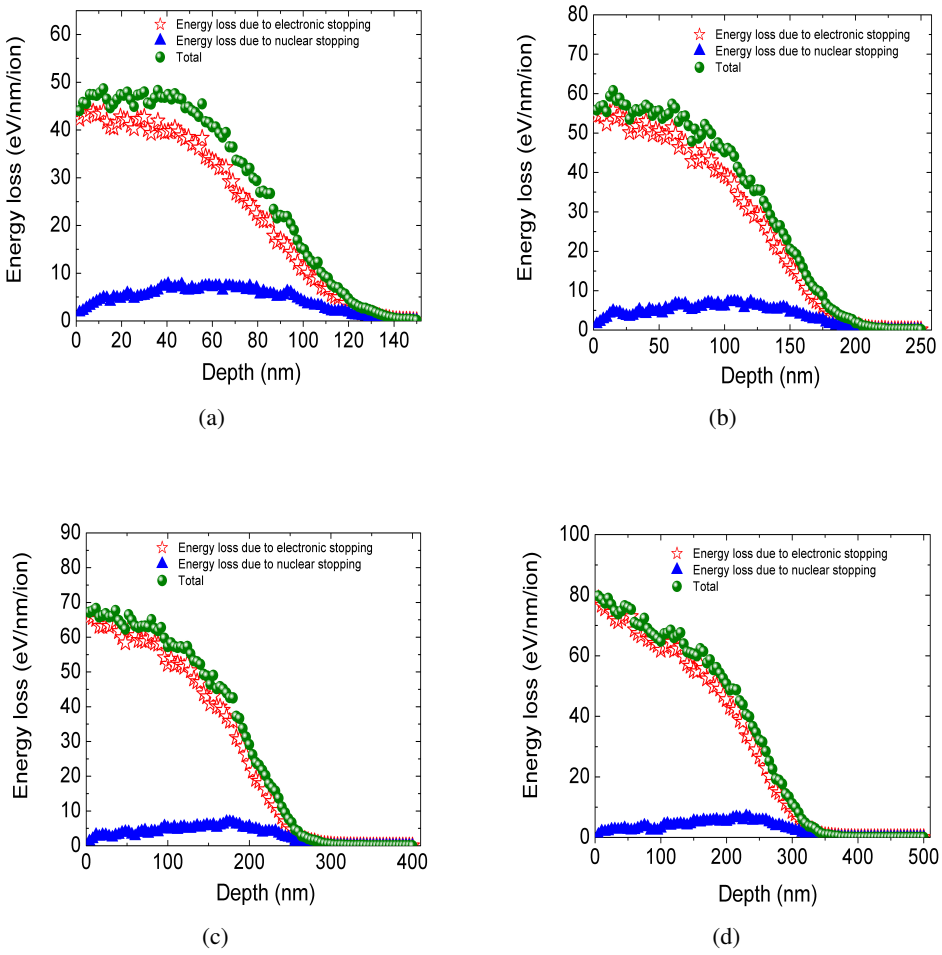

Figure 6.5: *Energy deposition of (a) 6-keV, (b) 10-keV, (c) 15-keV and (d) 20-keV Helium ions implanted into plasmid DNA calculated by the TRIM programme.*

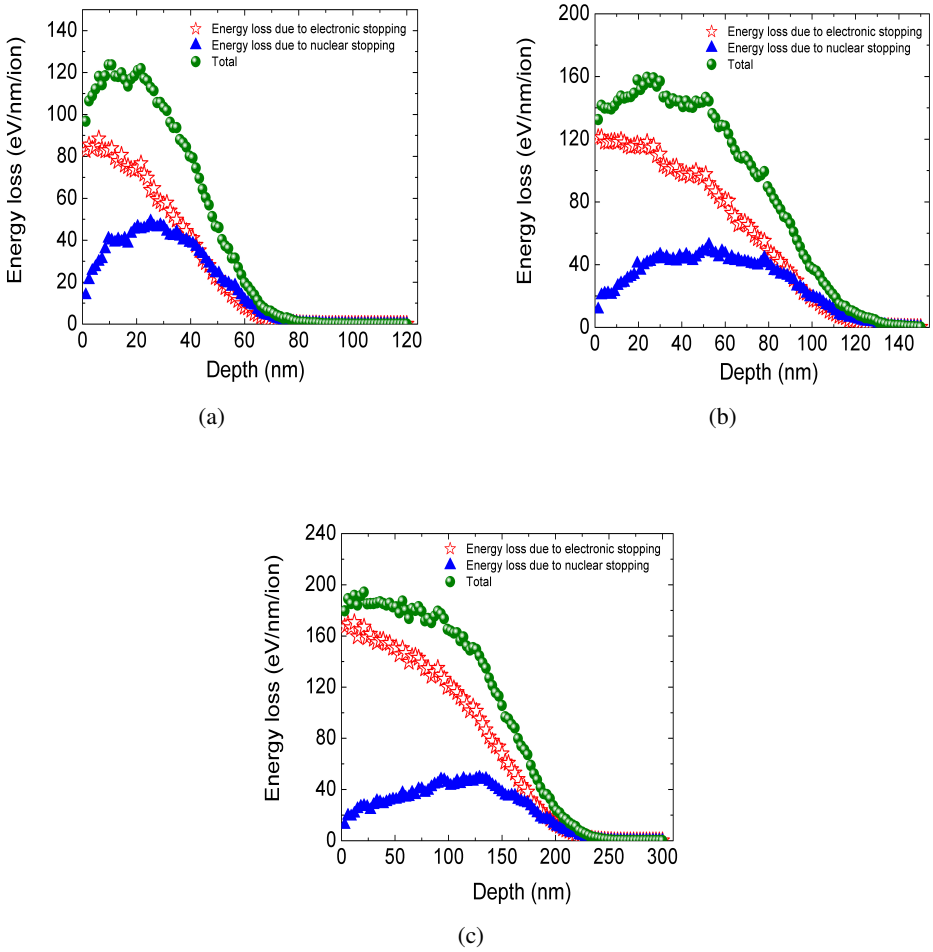

Figure 6.6: *Energy deposition of (a) 10-keV, (b) 20-keV, and (c) 40-keV Carbon ions implanted into plasmid DNA calculated by the TRIM programme.*

energy. In principle many processes may contribute such as ionization of plasmid constituents due to neutralization of the incoming ion or due to ion interaction with target valence electrons, direct dissociation of plasmids via dissociative states and knock out of atoms in direct impact or recoil cascades, the action of secondary electrons emitted along the ion trajectory or the much slower action of radicals produced in the film.

It has been suggested that the initial physical mechanisms in the energy loss process of low-energy heavy ions may be different from that of conventional ion irradiation where ionization and excitation play the most important role in producing DNA molecular lesions [59]. In the case of slow keV ions, the energy loss due to nuclear stopping can become more important than electron stopping. Particularly for heavy ions and lowest energies, it even dominates. This is due to an increasing cross section for binary atomic collisions with decreasing particle energy and due to increasing interaction times between ions and target atoms or molecules [164]. Thus low-energy ions can much more efficiently cause displacement of target atoms and the displaced atoms in turn may also displace other atoms [157]. This process may result in a collision cascade, leading to further local multiple damages, including bond breaks, molecular dissociation and fragment production [150, 165, 166].

In order to get an idea about the relevance of the direct atomic interactions we performed ion scattering simulations using the TRIM software package. The 'Transport of Ions in Matter' code [72] is a Monte Carlo approach to simulate the trajectories of ions penetrating into solids. Along the complete trajectory, TRIM keeps track of the energy transferred to electrons (electronic stopping) and atoms (nuclear stopping) of the target system. When a target atom receives sufficient recoil energy that its binding energy is overcome, the subsequent collision cascade is followed as well.

In TRIM, the target material is assumed to be amorphous. For plasmid DNA (pBR322), the number of adenine bases is 983, the number of guanine is 1134, the number of cytosine is 1210, and the number of thymine is 1034. It can be calculated that the average atom percentages are: 10.46% for N, 39.87% for H, 27.23% for C, 19.46% for O and 2.8% for P. The density is 1.46 g/cm^3 [167]. With these parameters, the depth distribution for energy loss due to electronic stopping and that due to nuclear stopping per nm are displayed in Fig. 6.4, 6.5 and 6.6 for the cases of H, He and C with different energy, respectively.

The shapes of the total energy loss curves are similar for all projectiles. However, the contributions of electronic and nuclear stopping are distinctively different for H, He, and C projectiles. For protons the energy loss is completely dominated by electronic energy loss. The nuclear stopping is on the order of 2 eV/nm, only. For He^{2+} ions the nuclear stopping amounts to approximately 5 – 8 eV/nm which is on the order of 10% of the total LET. For C ions nuclear stopping of up to 50 eV/nm is ob-

served, which is a substantial fraction ($\sim 30\%$) of the total energy loss. Here, nuclear stopping even dominates at the end of the ion trajectories.

The observed increased damage when going from H to He and from He to C is in line with the trends in nuclear energy loss as calculated using the TRIM code. Nuclear stopping describes direct energy transfer to target atoms.

If this energy exceeds atom binding energies, the atom is kicked out of the plasmid DNA molecule. This may be the starting point of a strand break. We therefore calculated the number of atomic displacements (vacancies) as a rough estimate for induced direct damage due to nuclear stopping.

It should be noted in this context that multiple damage could occur extending over a region of several tens of base pairs. Although this is an oversimplified approach to this complex problem, it is clear that important and fairly localized damage can occur by elastic energy transfer and recoils. A single strand break in the DNA can thus occur by, e.g. knocking a phosphorous atom out of the backbone. A double strand break can occur due to a successive collision of the incoming ion with atoms in the two strands or alternatively the second strand might be broken by recoiling atoms.

The result of the number of vacancies due to primary atomic displacements produced by different ions with various energy are shown in the figures 6.7, 6.8 and 6.9. For all ions under study, the vacany yield increases until it reaches a maximum at a certain depth before it decreases to zero at the end of the trajectories. The integrals of the vacancies produced for the ions and kinetic energies under study are compiled in the table 6.3. Results are given on a per ion and a per Gy basis. Vacancy yields between 2 and 10 per H^+ ion for kinetic energies between 0.5 keV and 20 keV are observed respectively. For He^{2+} between 6 keV and 20 keV, vacancy yields increase from 42 to 74 per ion. Due to their higher mass, He ions are more efficient in vacancy production. For C^{q+} ions, vacancy yields exceeding 100 per ion are observed, again increasing with kinetic energy. However, when looking at the results normalized to a per Gy basis, only a very weak dependence on the ion kinetic energy is left. Then, for protons of the order of 10^6 vacancies are induced per Gy whereas for He^{2+} about 8×10^6 vacancies are induced. For C ions, no further increase is observed!

This implies that the knock out of atoms alone, at least in the relatively crude model of an amorphous target, cannot explain the observed data alone. Comparing tables 6.3 and 6.2, we can recognize the strong increase in double strand breaks when going from H+ to He^{2+}. Vacancy production alone does not explain the strong increase in damage observed for C ions.

An explanation for this increase in damage could be the LET of C ions (see table 6.1) that is about 3 times larger as compared to He. Higher LET either implies denser events along each ion trajectory *or* more energetic secondary particles if number of events remains similar. In the first case, this could lead for instance to induction

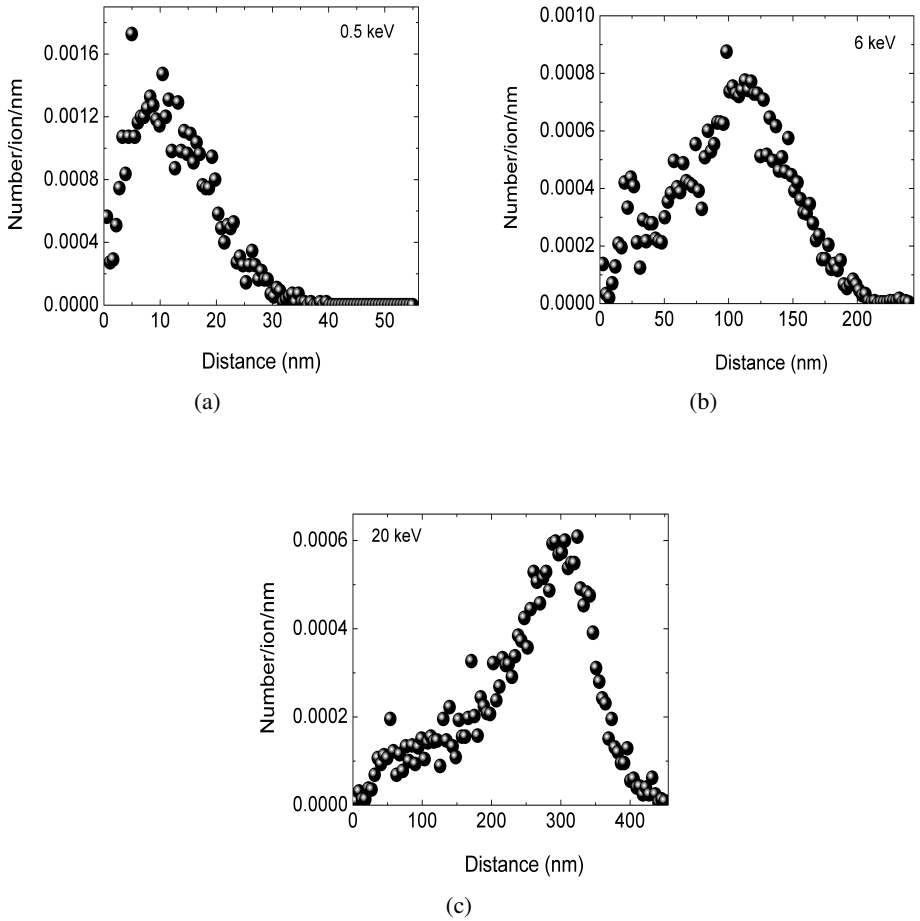

Figure 6.7: *Number of vacancies per nm created by incident H ions.*

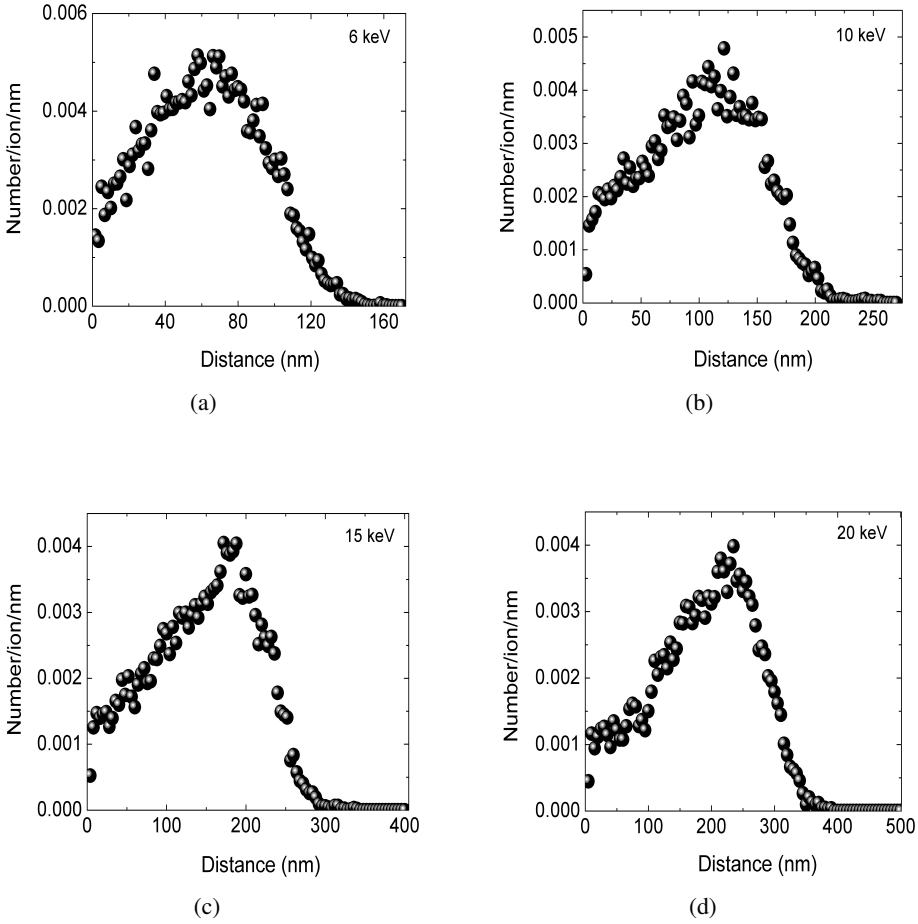

Figure 6.8: *Number of vacancies per nm created by incident He ions.*

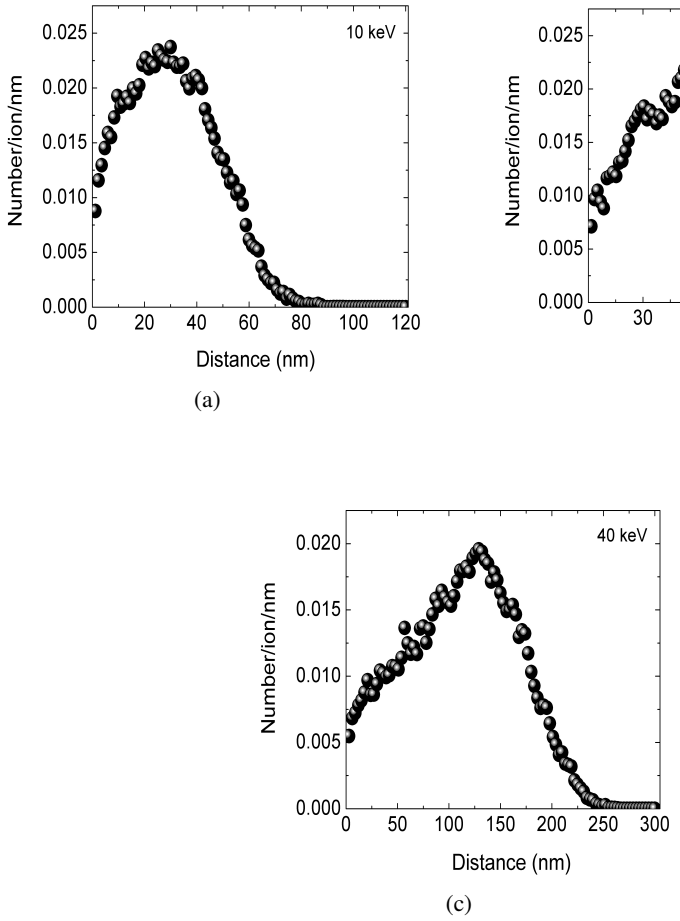

Figure 6.9: *Number of vacancies per nm created by incident C ions.*

Table 6.3: *Vacancies created in the thin film of plasmid DNA by ions beam*

Ion	Energy (keV)	Vacancies/ion	10^6 Vacancies/Gy
H	0.5	2	1
	6	8	1.5
	20	10	1.1
He	6	42	7
	10	55	8
	15	65	8.1
	20	74	8.2
C	10	110	5.2
	20	179	7.8
	40	270	10.8

of several adjacent SSB that lead to a DSB. In the second case, energetic recoil ions would potentially knock out neighboring atoms leading to additional DNA damage (secondary vacancies were not calculated here with the TRIM code).

6.4 Conclusion

In this chapter it is shown that keV ions can efficiently induce SSB and DSB in plasmid DNA thin films. Even though for a given ion kinetic energy, H^+ and He^{2+} ions have similar LETs, at identical dose about 5 times more DSBs are induced by He^{2+} ions. This finding hints at a strong contribution of nuclear stopping, since simulations showed that He^{2+} ions are about 5 times more efficient in direct atom knock out from the sample. For C^{q+} ions on the other hand, simulations predict very similar rates of vacancy production as compared to He^{2+}. However, DSB induction is found to increase by 1–2 orders of magnitude. We tentatively attribute this effect to the higher LET which could lead to increased complexity of local damage and higher DSB yields. Also, for C^{q+} ions, energetic recoils could induced further damage.

Thin film production, controlled irradiation and collection and analysis of the irradiated sample can be performed in a reproducible fashion. For the future, systematic studies on the influence of charge state and kinetic energy would certainly allow a deeper understanding on the damage process and in particular the interplay of electronic and nuclear stopping.